

Engineering nonreciprocal damping and polarization of spin waves in ferromagnetic domain wall via Dzyaloshinskii-Moriya interaction and spin-transfer torque

Xiang Liu(刘想), Xiguang Wang(王希光), Zhixiong Li(李志雄), Xiufeng Han(韩秀峰), and Guanghua Guo(郭光华)
Citation: Chin. Phys. B, 2026, 35 (**4**): 047502. DOI: 10.1088/1674-1056/ae2771
http://cpb.iphy.ac.cn; http://iopscience.iop.org/cpb

What follows is a list of articles you may be interested in

Stability and characteristic modes of skyrmions in magnetic nanotubes

Tijjani Abdulrazak, Qizhi Cai(蔡淇智), and Guangwei Deng(邓光伟)
Chin. Phys. B, 2025, 34 (**10**): 107512. DOI: 10.1088/1674-1056/ade071

Directly tunable magnon frequency comb effect based on domain wall

Xiaoxue Yang(杨霄雪), Huiting Li(李慧婷), Xue-Feng Zhang(张雪枫), Xiao-Ping Ma(马晓萍), Je-Ho Shim(沈帝虎), Yingjiu Jin(金迎九), and Hong-Guang Piao(朴红光)
Chin. Phys. B, 2025, 34 (**10**): 107507. DOI: 10.1088/1674-1056/ade856

Magnon behavior in YIG film under microwave excitation investigated by Brillouin light scattering

Guofu Xu(徐国服), Kang An(安康), Wenjun Ma(马文俊), Xiling Li(李喜玲), C. K. Ong, Chi Zhang(张驰), and Guozhi Chai(柴国志)
Chin. Phys. B, 2025, 34 (**6**): 067507. DOI: 10.1088/1674-1056/add24c

Orbital magnetic field effect on spin waves in a triangular lattice tetrahedral antiferromagnetic insulator

Pi-Ye Zhou(周丕烨), Xiao-Hui Li(李晓慧), and Yuan Wan(万源)
Chin. Phys. B, 2025, 34 (**6**): 067501. DOI: 10.1088/1674-1056/adca1f

Strain-manipulated dispersion characteristics of magnonic crystals with Dzyaloshinskii-Moriya interaction and applications on spin-wave devices

Chuhan Zhou(周楚涵), Xiaotian Jiao(焦晓天), Jiaxi Xu(徐佳熙), Zhaonian Jin(金兆年), Lin Chen(陈琳), and Zhikuo Tao(陶志阔)
Chin. Phys. B, 2025, 34 (**2**): 027501. DOI: 10.1088/1674-1056/ad9892

SPECIAL TOPIC — Advanced magnonics

Engineering nonreciprocal damping and polarization of spin waves in ferromagnetic domain wall via Dzyaloshinskii–Moriya interaction and spin-transfer torque

Xiang Liu(刘想)[1], Xiguang Wang(王希光)[1,†], Zhixiong Li(李志雄)[1], Xiufeng Han(韩秀峰)[2], and Guanghua Guo(郭光华)[1,‡]

[1] *School of Physics, Central South University, Changsha* 410083, *China*

[2] *Beijing National Laboratory for Condensed Matter Physics, Institute of Physics, Chinese Academy of Sciences, Beijing* 100190, *China*

(Received 26 October 2025; revised manuscript received 24 November 2025; accepted manuscript online 3 December 2025)

Manipulation of spin-wave polarization is fundamental for designing novel magnonic devices based on the polarization coding technique. Here, we demonstrate the generation of left-handed polarized spin waves (LPSWs) in a ferromagnetic domain wall and their polarization modulation through the combined effect of the Dzyaloshinskii–Moriya interaction (DMI) and spin-polarized electric current. A phase diagram delineating the stability regions of left- and right-handed polarized spin waves (RPSWs) is constructed as a function of DMI strength and current density. Our results reveal a pronounced DMI-induced nonreciprocal damping effect, predominantly manifested in RPSWs while leaving LPSWs largely unaffected. This phenomenon enables effective filtering of RPSWs in one direction, allowing the realization of pure LPSW propagation as well as elliptically polarized spin waves with tunable eccentricity. Our work provides a viable method for controlling spin-wave polarization and nonreciprocal propagation in ferromagnetic systems.

Keywords: spin wave, Dzyaloshinskii–Moriya interaction, spin-polarized electric current, ferromagnetic domain wall

PACS: 75.60.Ch, 85.75.–d, 75.40.Gb

DOI: 10.1088/1674-1056/ae2771 **CSTR:** 32038.14.CPB.ae2771

1. Introduction

Magnonics has garnered significant interest due to the numerous advantages of magnon-based devices over traditional electronic systems, including energy-efficient information transmission without Joule heating, broad operational bandwidth spanning GHz to THz frequencies, and nanoscale component integration.[1–9] Based on the modulation of the amplitude and phase of spin waves (SWs), various magnonic devices have been developed, such as amplitude encoders, phase encoders, transducers, magnonic transistors, and related logic gates.[10–15] However, functional devices based on SW polarization are still limited to antiferromagnets and ferrimagnets.[16–18] This limitation arises from the presence of two magnetic sublattices with antiparallel magnetization in antiferromagnets and ferrimagnets, naturally giving rise to two types of polarized SW modes: left-handed polarized SWs (LPSWs) and right-handed polarized SWs (RPSWs). In contrast, in ferromagnets, only RPSWs exist, and magnonic devices based on polarization modulation have not yet been realized. In our earlier works,[19,20] we demonstrated that LPSWs can be induced in ferromagnets by spin transfer torque (STT), coexisting with RPSWs to form elliptically polarized SWs. While pure LPSWs have not yet been realized in ferromagnets, this limitation hinders, to a certain extent, the implementation of polarization-encoded magnonic devices.

Nonreciprocal propagation of SWs is important for designing functional magnonic devices.[21–24] The Dzyaloshinskii–Moriya interaction (DMI) is a type of exchange interaction characterized by its chiral nature.[25–28] Consequently, DMI naturally induces nonreciprocal propagation of SWs. The DMI-induced SW nonreciprocity is reflected in a term linear in the wave vector k in the SW dispersion relation, resulting in asymmetric phase, velocity, attenuation length, etc., of SWs propagating in opposite directions.[29–34] DMI also gives rise to SW damping nonreciprocity,[35] meaning SWs propagating in opposite directions experience different damping constants, which is especially significant in the low-frequency range. Thus, the DMI-induced nonreciprocal damping effect can be clearly observed in magnetic domain walls (DWs), where the SW cutoff frequency is zero. To date, DMI-induced SW nonreciprocity has been widely exploited to design novel magnonic devices.[5,7,36–38] It is also worth noting that the DMI-induced linear shift of SW dispersion is similar to the SW Doppler shift induced by spin-polarized electric currents. As a result, the critical current

†Corresponding author. E-mail: wangxiguang@csu.edu.cn

‡Corresponding author. E-mail: guogh@mail.csu.edu.cn

© 2026 Chinese Physical Society and IOP Publishing Ltd. All rights, including for text and data mining, AI training, and similar technologies, are reserved.

required to generate LPSWs in ferromagnets can be significantly reduced in the presence of DMI.[19] Additionally, the interplay between DMI and strain can manipulate SW dispersions in magnonic crystals.[39] DMI also induces non-zero Berry curvature and leads to the thermomagnonic Hall effect in checkerboard ferromagnets.[40]

Here, we study the propagation and manipulation of SWs in a ferromagnetic DW under the combined effect of DMI and spin-polarized electric current. LPSWs are produced by STT. Interestingly, the DMI-induced damping nonreciprocity differs for LPSWs and RPSWs; this effect can be utilized to filter out RPSWs, achieving pure LPSW propagation in a target direction. The SW phase diagram is plotted as a function of DMI strength and current density, and the analytical results are verified by micromagnetic simulations.

2. Model and method

The model considered here is a Bloch DW in a thin ferromagnetic film with perpendicular magnetic anisotropy, as shown in Fig. a. The equilibrium magnetization at the DW center is directed along the x axis. The SWs propagating in the DW are governed by the Landau–Lifshitz–Gilbert (LLG) equation

$$\begin{aligned}\frac{\partial \boldsymbol{m}}{\partial t} &= -\gamma \boldsymbol{m}\times \boldsymbol{H}_{\rm eff} + \alpha \boldsymbol{m}\times\frac{\partial \boldsymbol{m}}{\partial t}\\ &\quad -c_j \boldsymbol{m}\times\left(\boldsymbol{m}\times\frac{\partial \boldsymbol{m}}{\partial x}\right) - \beta c_j \boldsymbol{m}\times\frac{\partial \boldsymbol{m}}{\partial x},\end{aligned} \tag{1}$$

where $\boldsymbol{m}=\boldsymbol{M}/M_{\rm s}$ is the unit vector of the magnetization, γ is the gyromagnetic ratio, and α is the Gilbert damping constant. $c_j = P j_e \mu_{\rm B}/\left[eM_{\rm s}\left(1+\beta^2\right)\right]$ is the STT coefficient, where j_e is the current density, $\mu_{\rm B}$ is the Bohr magneton, P is the spin polarization of the current, e is the electron charge, and β is the nonadiabatic torque coefficient. The effective field is defined as $\boldsymbol{H}_{\rm eff} = -\delta E/(\mu_0 \delta \boldsymbol{M})$. The free energy E includes the exchange interaction, uniaxial anisotropy, demagnetization energy, and bulk DMI.[7,41] Therefore, the effective field can be expressed as

$$\boldsymbol{H}_{\rm eff} = q\nabla^2 \boldsymbol{m} + H_{\rm K}\left(\boldsymbol{m}\cdot\boldsymbol{e}_z\right)\boldsymbol{e}_z + \boldsymbol{H}_{\rm d} - D_{\rm b}\left(\nabla\times\boldsymbol{m}\right), \tag{2}$$

with $q = 2A/(\mu_0 M_{\rm s})$, $H_{\rm K} = 2K_{\rm eff}/(\mu_0 M_{\rm s})$, $K_{\rm eff} = K - \mu_0 M_{\rm s}^2/2$, and $D_{\rm b} = 2D/(\mu_0 M_{\rm s})$. Here, A is the exchange constant, D is the DMI constant, and K is the anisotropy constant. The demagnetization field is given by $\boldsymbol{H}_{\rm d} = -N_y M_{\rm s}(\boldsymbol{m}\cdot\boldsymbol{e}_y)\boldsymbol{e}_y$.[42] Here, $N_y = d/(d+\pi\Delta)$, where d is the thickness of the film and $\Delta = \sqrt{A/K_{\rm eff}}$ is the characteristic width of the DW.

Consider a small perturbation around the static equilibrium, the unit magnetization vector can be expressed as $\boldsymbol{m}_{\rm r} = (m_{\rm r}, m_\theta, m_\phi)$ in spherical coordinates, where θ and ϕ represent the polar and azimuthal angles, respectively. m_θ and m_ϕ are small perturbations that deviate from the equilibrium state in the presence of SWs, and $m_{\rm r}=1$ under the linear approximation. The equilibrium Bloch DW is approximated by the Walker profile $\tan(\theta/2) = \exp(\pm y/\Delta)$, $\phi = 0$.[43] The partial differential equations describing SWs in the DW are obtained by linearizing Eq. (1)

$$\begin{cases}\dfrac{\partial m_\theta}{\partial t} = \left\{\gamma q\nabla^2 - \gamma H_{\rm K}\left[1-2\,{\rm sech}^2\left(\dfrac{y}{\Delta}\right)\right] - \alpha\dfrac{\partial}{\partial t} + \beta c_j\dfrac{\partial}{\partial x} - \gamma N_y M_{\rm s} \mp \dfrac{\gamma D_{\rm b}}{\Delta}{\rm sech}\left(\dfrac{y}{\Delta}\right)\right\} m_\varphi + \left[c_j - \gamma D_{\rm b}{\rm sech}\left(\dfrac{y}{\Delta}\right)\right]\dfrac{\partial m_\theta}{\partial x},\\ \dfrac{\partial m_\varphi}{\partial t} = \left\{-\gamma q\nabla^2 + \gamma H_{\rm K}\left[1-2\,{\rm sech}^2\left(\dfrac{y}{\Delta}\right)\right] + \alpha\dfrac{\partial}{\partial t} - \beta c_j\dfrac{\partial}{\partial x}\right\} m_\theta + \left[c_j - \gamma D_{\rm b}{\rm sech}\left(\dfrac{y}{\Delta}\right)\right]\dfrac{\partial m_\varphi}{\partial x}.\end{cases} \tag{3}$$

The SW solutions in DWs can be assumed as[44]

$$\begin{cases} m_\theta = m_{\theta 0}\exp\left[{\rm i}(\omega t - kx)\right]{\rm sech}(\dfrac{y}{\Delta}),\\ m_\varphi = m_{\varphi 0}\exp\left[{\rm i}(\omega t - kx)\right]{\rm sech}(\dfrac{y}{\Delta}).\end{cases} \tag{4}$$

Substituting Eq. (4) into Eq. (3) and treating the effect of DMI as a perturbation term,[31,45] one obtains the SW dispersion relation and imaginary frequency

$$\begin{aligned}\omega_{\rm rL} &= -\gamma\sqrt{qk^2\left(qk^2 + N_y M_{\rm s} + \frac{\pi|D_{\rm b}|}{4\Delta}\right)}\\ &\quad + \left(\frac{\pi}{4}\gamma D_{\rm b} - c_j\right)k,\\ \omega_{\rm rR} &= \gamma\sqrt{qk^2\left(qk^2 + N_y M_{\rm s} + \frac{\pi|D_{\rm b}|}{4\Delta}\right)}\\ &\quad + \left(\frac{\pi}{4}\gamma D_{\rm b} - c_j\right)k,\end{aligned} \tag{5}$$

$$\omega_{\rm iL(R)} = \frac{\gamma\left(\alpha\omega_{\rm rL(R)} + \beta c_j k\right)\left(qk^2 + \dfrac{N_y M_{\rm s}}{2} + \dfrac{\pi|D_{\rm b}|}{8\Delta}\right)}{\omega_{\rm rL(R)} - \left(\dfrac{\pi\gamma D_{\rm b}}{4} - c_j\right)k}. \tag{6}$$

Here, $\omega_{\rm rL}$ and $\omega_{\rm rR}$ represent the dispersions of LPSW and RPSW, respectively, and $\omega_{\rm iL}$ and $\omega_{\rm iR}$ denote the imaginary frequencies of LPSW and RPSW, respectively.

For numerical calculations, the magnetic parameters corresponding to the L10-ordered $Fe_{50}Pd_{50}$ (001) film are used:[46] $M_{\rm s} = 1$ MA/m, $A = 15$ pJ/m, and $K = 1$ MJ/m^3. The Gilbert damping constant $\alpha = 0.01$ is adopted to ensure proper SW propagation. The nonadiabatic STT coefficient is taken as $\beta = 0.014$. Full micromagnetic simulations are performed using MuMax3[47] to verify the theoretical predictions. The fer-

romagnetic film with a Bloch DW is discretized into a $2200 \times 61 \times 1$ grid with cell size 2 nm $\times$ 2 nm $\times$ 1 nm. An absorbing boundary condition is applied to eliminate the influence of reflected SWs.[48] To simulate the SW dispersion spectrum, a sinc-shaped magnetic pulse $h(t) = he_y \sin(2\pi f_c t)/(2\pi f_c t)$ is used, with $h = 10$ mT and $f_c = 50$ GHz. The time evolution of m_y is monitored at all cells located at the DW center for a duration of 50 ns, with a discrete time step of 10 ps. The SW dispersion relationships are obtained using a spatiotemporal fast Fourier transform.

3. Results and discussion

The occurrence of STT-induced LPSW is determined by the condition that the maximum frequency of the LPSW dispersion should be larger than zero, i.e., $\omega_{\text{rL-max}} > 0$,[19] which gives the critical coefficient c_{je} derived from Eq. (5)

$$c_{je} = \pm\gamma\sqrt{q\left(N_y M_s + \frac{\pi|D_b|}{4\Delta}\right)} + \frac{\pi}{4}\gamma D_b, \tag{8}$$

Here, the positive and negative signs ($\pm$) correspond to the cases where the signs of c_j and D_b are the same and opposite, respectively. Specifically, if D_b is positive, when the STT coefficient c_j is also positive, the sign of the first term on the right-hand side of Eq. (8) is positive; if c_j is negative, the first term is negative. Therefore, the DMI can reduce the critical current density for the generation of LPSW if the signs of c_j and D_b are opposite. Equation (8) also indicates that the demagnetization factor N_y can affect the critical current density. N_y reflects the DW structure, and a large DW width in a thin film is beneficial for reducing the critical current density. Therefore, in experiments, it is recommended to use wider DWs in thin films with larger DMI to reduce the critical current density.

The STT also leads to instability of the system, which occurs when $\omega_{\text{iL(R)-min}} < 0$.[49–52] The critical coefficient c_{js} at the onset of instability is obtained from Eq. (7)

$$c_{js} = \pm\frac{\alpha}{|\alpha-\beta|}\gamma\sqrt{q\left(N_y M_s + \frac{\pi|D_b|}{4\Delta}\right)} + \frac{\alpha}{\alpha-\beta}\frac{\pi}{4}\gamma D_b. \tag{9}$$

Here, the signs ($\pm$) of the first term on the right-hand side of Eq. (9) have the same meaning as in Eq. (8). As $|c_{je}| < |c_{js}|$, stable LPSWs can exist in DWs if the current satisfies $|c_{je}| < |c_j| < |c_{js}|$.

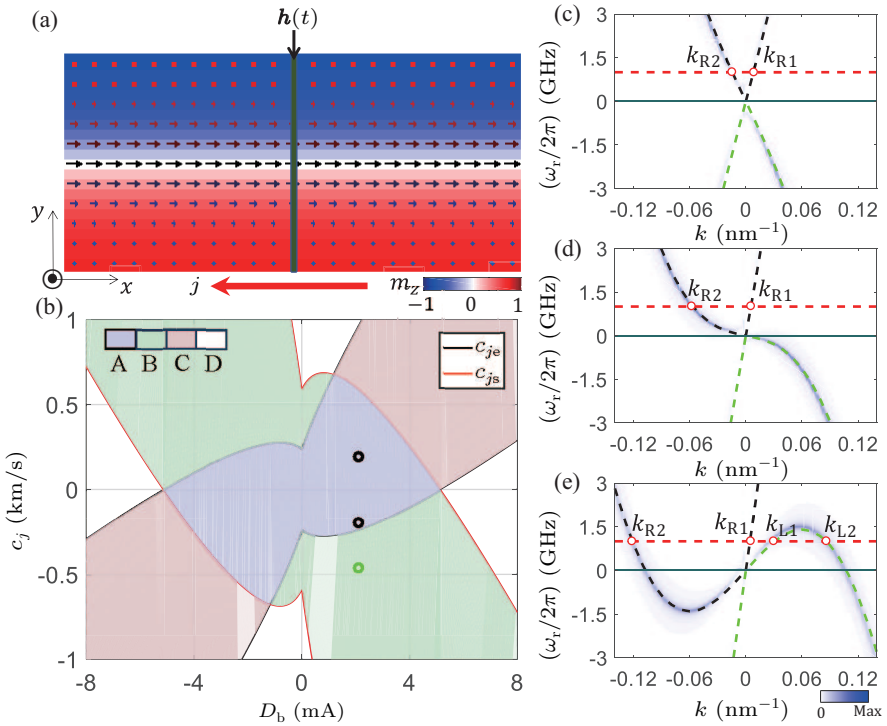


Fig. 1. Schematic of the Bloch DW in a thin ferromagnetic film with perpendicular anisotropy. The arrows represent the direction of the static magnetization. (b) Phase diagram for the stable LPSW and RPSW states and SW instability determined by the strength of DMI and current density. In region A only RPSW exists, in region B LPSW and RPSW coexist, and in regions C and D the system becomes unstable. (c)–(e) Dispersions of SWs for (c) $c_j = 0.19$ km/s, (d) $c_j = -0.19$ km/s, and (e) $c_j = -0.46$ km/s. In all cases, $D_b = 2.1$ mA ($D = 1.3$ mJ/m^2). The green and black dashed lines are the analytically calculated dispersions, and the bright background color represents the simulated results. The red dashed line and cyan solid line indicate $\omega/(2\pi) = 1$ GHz and $\omega/(2\pi) = 0$, respectively.

Based on the two critical currents c_{je} and c_{js} given in Eqs. (8) and (9), we plot the phase diagram for the stable LPSW and RPSW states and SW instability determined by the strength of DMI and current density, which is shown in Fig. 1(b). The critical current curves c_{je} and c_{js} divide the $D_b \sim c_j$ space into four regions. In region A, with small current and weak DMI, only the RPSWs exist. Typical SW dispersions in region A are given in Figs. 1(c) and 1(d). The

LPSW dispersion is below the abscissa, indicating that only stable RPSWs can be hosted in the domain wall. The difference in SW dispersions between Figs. 1(c) and 1(d) arises from the fact that the effects of DMI and STT cancel each other in Fig. 1(c), while they are enhanced in Fig. 1(d). In region B, the stable LPSW can be induced by STT and coexists with the RPSW. The corresponding SW dispersions are presented in Fig. 1(e). Here, the STT and DMI push the LPSW dispersion curve across the horizontal axis, generating LPSWs with positive frequency. The stable LPSWs exist when the wave vector k is limited in the range

$$0 < k < \sqrt{\frac{(\gamma\pi D_{\rm b} - 4c_j)^2}{(4\gamma q)^2} - \frac{N_y M_{\rm s}}{q} - \frac{\pi |D_{\rm b}|}{4q\Delta}},$$

for $D_{\rm b} > 0$ and $c_j < 0$. In regions C and D, the condition for the onset of instability given by Eq. (9) is satisfied, and SWs become unstable.

To further demonstrate the characteristics of the LPSW and RPSW modes, we excite the SWs using a harmonic field $h(t) = he_y \cos(2\pi ft)$ with $h = 1$ mT and $f = 1$ GHz (indicated by the red lines in Figs. 1(c)–1(e)), and simulate the SW propagation in the DW. The results are presented in Fig. 2. Figures 2(a) and 2(b) show the propagation profiles of SWs in region A (two points indicated by black dots in Fig. 1(b)), and the corresponding spatial Fourier transforms are presented in Figs. 2(d) and 2(e). Here, only the RPSWs are excited. The right-moving RPSW with wave vector $k_{\rm R1}$ is significantly weaker than the left-moving RPSW with wave vector $k_{\rm R2}$, reflecting strong damping nonreciprocity. Reversing the direction of the current, the damping nonreciprocity feature is almost the same, indicating that the STT-induced SW damping has a weak effect as it depends on the current direction.[53] This damping nonreciprocity of SWs in DWs is induced by the DMI.[35] It is worth noting that the DMI-induced nonreciprocal damping has been verified experimentally.[54] In region B (a point represented by the green dot in Fig. 1(b)), both LPSWs and RPSWs are simultaneously stimulated as shown in Fig. 2(c). Here, the strength of the RPSW propagating to the right ($k_{\rm R1}$) is significantly smaller than that of the RPSW propagating to the left ($k_{\rm R2}$) (see Fig. 2(f)), demonstrating the DMI-induced nonreciprocal damping. In contrast, the strengths of the two LPSWs propagating to the left ($k_{\rm L2}$) and right ($k_{\rm L1}$) are comparable, indicating that the DMI-induced damping nonreciprocity is not manifested on the LPSWs. Due to the difference in damping nonreciprocity between the LPSW and RPSW, the SW propagating to the left in Fig. 2(c) is a superposition of the LPSW ($k_{\rm L2}$) and RPSW ($k_{\rm R2}$), and the trajectory of magnetization precession is an ellipse with large eccentricity. Conversely, the SW propagating to the right is nearly a pure LPSW, and the trajectory is a circle with left-handed precession. Thus, we achieve pure LPSWs in ferromagnets, and the propagation direction of the pure LPSW can be reversed by switching the chirality of DMI and the direction of the spin-polarized electric current.

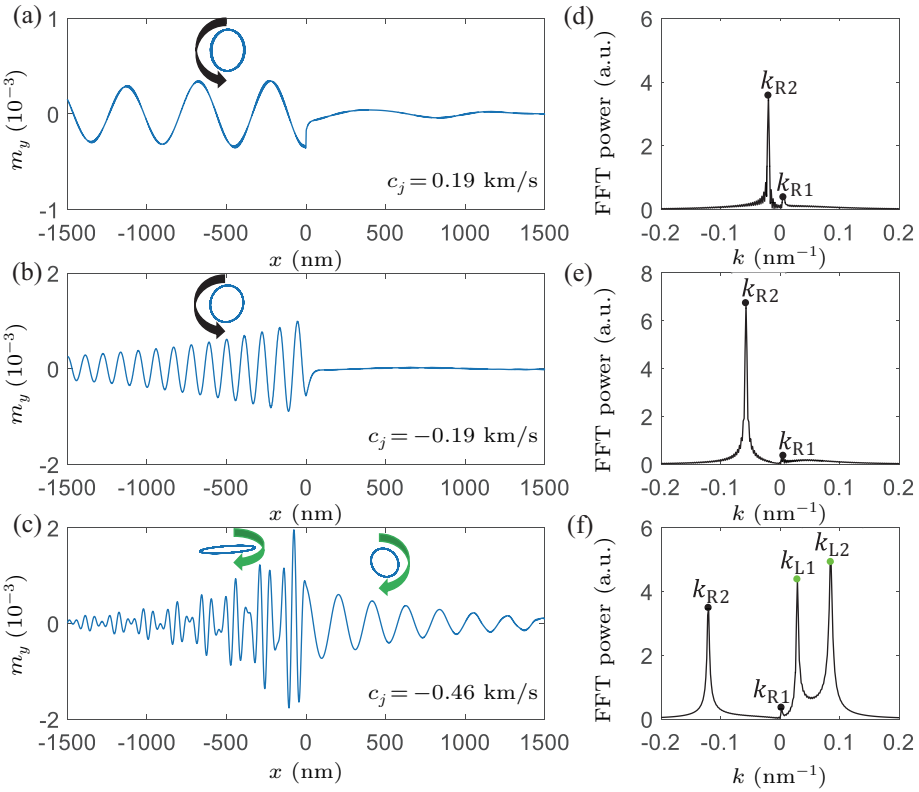


Fig. 2. (a)–(c) Propagation profiles of SWs propagating in the DW for (a) $c_j = 0.19$ km/s, (b) $c_j = -0.19$ km/s, and (c) $c_j = -0.46$ km/s. (d)–(f) Corresponding spatial Fourier transformations of (a)–(c). In all cases, $D_{\rm b} = 2.1$ mA ($D = 1.3$ mJ/m^2).

To clarify the different manifestations of the damping nonreciprocity on the LPSW and RPSW, we analyze the imaginary frequency of SWs given by Eq. (7) and calculate its dependence on the wave vector k, which is presented in Fig. 3. It shows that both the LPSW and RPSW display obvious nonreciprocity of the imaginary frequency for positive and negative k, while the chirality of nonreciprocity is opposite. The nonreciprocity is more significant for small k, and a jump occurs as $k \to 0$. Therefore, both the RPSW and LPSW exhibit nonreciprocal damping. This nonreciprocity, however, is determined by the sign of the wave vector k rather than the direction of SW propagation. As shown in Fig. 1(e), the two excited RPSWs have wave vectors of opposite signs and propagate in opposite directions. In contrast, although the two LPSWs also travel in opposite directions, their wave vectors have the same sign. Consequently, the damping nonreciprocity is not observed clearly in the LPSWs.

Exploiting STT-generated LPSWs and the DMI-induced damping nonreciprocity, we can not only obtain pure LPSWs but also modulate the SW polarization. Figure 4 shows the trajectories of the magnetization precession at site $x = -500$ nm under different current densities. We see that, when $c_j = -0.44$ km/s, the magnetization precession is RPSW-dominated right-handed elliptical. At $c_j = -0.46$ km/s, the precession trajectory is LPSW-dominated left-handed elliptical. When c_j increases to -0.49 km/s, the SW becomes nearly linearly polarized. Thus, by varying the current density, we can modulate SW elliptical polarization with tunable eccentricity.

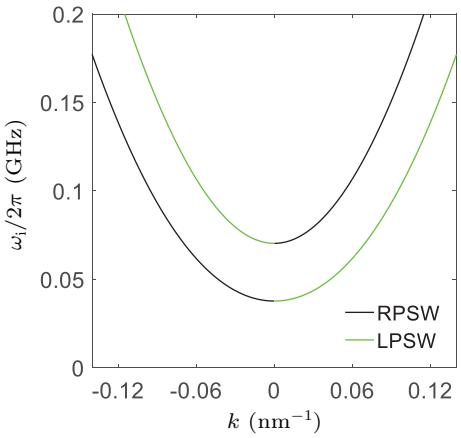


Fig. 3. Imaginary frequency of SWs as a function of the wave vector k. The parameters are $c_j = -0.46$ km/s and $D_b = 2.1$ mA ($D = 1.3$ mJ/m^2).

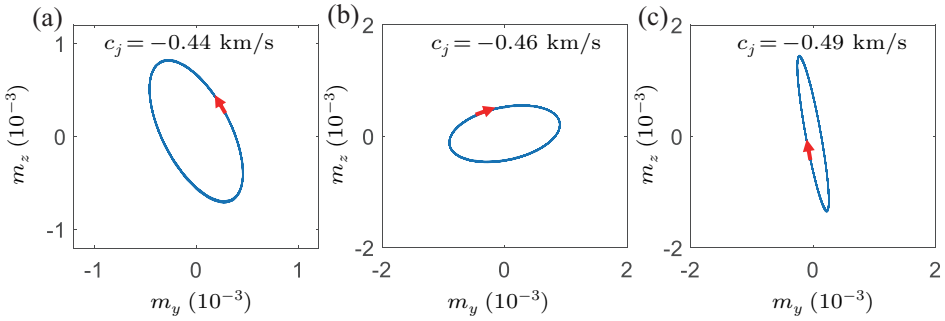


Fig. 4. Precession trajectories of the magnetization at site $x = -500$ nm for different current densities: (a) $c_j = -0.44$ km/s, (b) $c_j = -0.46$ km/s, and (c) $c_j = -0.49$ km/s. In all cases, $D_b = 1.6$ mA ($D = 1$ mJ/m^2).

4. Summary

We theoretically investigate SWs and their manipulation in ferromagnetic DWs through the interplay of the DMI and STT. We demonstrate the emergence of LPSWs and construct a phase diagram depicting the stable existence regions for LPSWs and RPSWs. A DMI-induced nonreciprocal damping of SWs for positive and negative wave vectors is observed. This damping nonreciprocity is predominantly manifested in RPSWs, while its effect on LPSWs is negligible. The asymmetry arises because two RPSWs propagating in opposite directions have opposite signs of the wave vector, whereas the DMI-induced LPSWs share the same wave vector signs despite propagating in opposite directions. This feature enables the generation of pure LPSWs in a desired direction, as well as elliptically polarized SWs with tunable eccentricity. Our work provides an effective approach for controlling SW polarization and may be utilized in designing magnonic devices based on polarization coding techniques.

Acknowledgments

This work is supported by the National Natural Science Foundation of China (Grant Nos. T2495212, 12274469, 12074437, and 12174452) and the Natural Science Foundation of Hunan Province of China (Grant Nos. 2025JJ20005 and 2023JJ40694). We also acknowledge computational resources provided by the High-Performance Computing Center of Central South University.

References

[1] Kruglyak V V, Demokritov S O and Grundler D 2010 *J. Phys. D: Appl. Phys.* **43** 264001

[2] Chumak A V, Vasyuchka V I, Serga A A and Hillebrands B 2015 *Nat. Phys.* **11** 453

[3] Serga A A, Chumak A V and Hillebrands B 2010 *J. Phys. D: Appl. Phys.* **43** 264002

[4] Lenk B, Ulrichs H, Garbs F and Münzenberg M 2011 *Phys. Rep.* **507** 107
[5] Barman A, Gubbiotti G, Ladak S, *et al.* 2021 *J. Phys.: Condens. Matter.* **33** 413001
[6] Pirro P, Vasyuchka V I, Serga A A and Hillebrands B 2021 *Nat. Rev. Mater.* **6** 1114
[7] Yu H M, Xiao J and Schultheiss H 2021 *Phys. Rep.* **905** 1
[8] Zenbaa N, Abert C, Majcen F, Kerber M, Serha R O, Knauer S, Wang Q, Schrefl T, Suess D and Chumak A V 2025 *Nat. Electron.* **8** 106
[9] Lan G B, Liu K Y, Wang Z Y, Xia F, Xu H J, Guo T Y, Zhang Y, He B, Li J H, Wan C H, Bauer G E W, Yan P, Liu G Q, Pan X Y, Han X F and Yu G Q 2025 *Nat. Commun.* **16** 1178
[10] Kostylev M P, Serga A A, Schneider T, Leven B and Hillebrands B 2005 *Appl. Phys. Lett.* **87** 153501
[11] Khitun A and Wang K L 2005 *Superlatt. Microstruct.* **38** 184
[12] Chumak A V, Serga A A and Hillebrands B 2014 *Nat. Commun.* **5** 4700
[13] Au Y, Ahmad E, Dmytriiev O, Dvornik M, Davison T and Kruglyak V V 2012 *Appl. Phys. Lett.* **100** 182404
[14] Schneider T, Serga A A, Leven B, Hillebrands B, Stamps R L and Kostylev M P 2008 *Appl. Phys. Lett.* **92** 022505
[15] Klingler S, Pirro P, Brächer T, Leven B, Hillebrands B and Chumak A V 2015 *Appl. Phys. Lett.* **106** 212406
[16] Yu W C, Lan J and Xiao J 2020 *Phys. Rev. Appl.* **13** 024055
[17] Cheng R, Daniels M W, Zhu J G and Xiao D 2016 *Sci. Rep.* **6** 24223
[18] Zhang Y, Feng X Q, Zheng Z Y, Zhang Z Z, Lin K L, Sun X H, Wang G D, Wang J K, Wei J Q, Vallobra P, He Y, Wang Z X, Chen L, Zhang K, Xu Y and Zhao W S 2023 *Appl. Phys. Rev.* **10** 011301
[19] Zhou Z W, Wang X G, Nie Y Z, Xia Q L, Zeng Z M and Guo G H 2019 *Phys. Rev. B* **99** 014420
[20] Liu X, Wang X G, Li Z X and Guo G H 2024 *Acta Phys. Sin.* **73** 147501 (in Chinese)
[21] Ye X Y, Xia K, Bauer G E W and Yu T 2024 *Phys. Rev. Applied* **22** L011001
[22] Liu X 2025 *J. Magn. Magn. Mater.* **627** 173121
[23] Xue Z P, Zou J, Cai C Y, Bauer G E W and Yu T 2025 *Phys. Rev. B* **112** 094438
[24] Zhou X H, Ye X Y and Yu T 2025 *Phys. Rev. Applied* **24** 034055
[25] Dzyaloshinsky I 1958 *J. Phys. Chem. Solids* **4** 241
[26] Moriya T 1960 *Phys. Rev.* **120** 91
[27] Yang H X, Thiaville A, Rohart S, Fert A and Chshiev M 2015 *Phys. Rev. Lett.* **115** 267210
[28] Zhang W J, Wei F, Liu B, Zhou Y, Kang S S and Sun B 2024 *Chin. Phys. B* **33** 048501
[29] Moon J H, Seo S M, Lee K J, Kim K W, Ryu J, Lee H W, McMichael R D and Stiles M D 2013 *Phys. Rev. B* **88** 184404
[30] Cortés-Ortuño D and Landeros P 2013 *J. Phys.: Condens. Matter.* **25** 156001
[31] Garcia-Sanchez F, Borys P, Soucaille R, Adam J P, Stamps R L and Kim J V 2015 *Phys. Rev. Lett.* **114** 247206
[32] Wang H C, Chen J L, Liu T, Zhang J Y, Baumgaertl K, Guo C Y, Li Y H, Liu C P, Che P, Tu S, Liu S, Gao P, Han X F, Yu D P, Wu M Z, Grundler D and Yu H M 2020 *Phys. Rev. Lett.* **124** 027203
[33] Kostylev M 2014 *J. Appl. Phys.* **115** 233902
[34] Zingsem B W, Farle M, Stamps R L and Camley R E 2019 *Phys. Rev. B* **99** 214429
[35] Liu X, Li Z X, Wang X G and Guo G H 2024 *J. Magn. Magn. Mater.* **610** 172556
[36] Lan J, Yu W, Wu R and Xiao J 2015 *Phys. Rev. X* **5** 041049
[37] Flebus B, Grundler D, Rana B, Otani Y, Barsukov I, Barman A, Gubbiotti G, Landeros P, Akerman J, Ebels U, Pirro P, Demidov V E, Schultheiss K, Csaba G, Wang Q, Ciubotaru F, Nikonov D E, Che P, Hertel R, Ono T, Afanasiev D, Mentink J, Rasing T, Hillebrands B, Kusminskiy S V, Zhang W, Du C R, Finco A, van der Sar T, Luo Y K, Shiota Y, Sklenar J, Yu T and Rao J W 2024 *J. Phys.: Condens. Matter.* **36** 363501
[38] Petti D, Tacchi S and Albisetti E 2022 *J. Phys. D: Appl. Phys.* **55** 293003
[39] Zhou C H, Jiao X T, Xu J X, Jin Z N, Chen L and Tao Z K 2025 *Chin. Phys. B* **34** 027501
[40] Zhu H, Shi H C, Tang Z G, and Tang B 2024 *Chin. Phys. B* **33** 037503
[41] Lu J, Li M and Wang X R 2020 *Phys. Rev. B* **101** 134431
[42] Mougin A, Cormier M, Adam J P, Metaxas P J and Ferré J 2007 *Europhys. Lett.* **78** 57007
[43] Schryer N L and Walker L R 1974 *J. Appl. Phys.* **45** 5406
[44] Winter J M 1961 *Phys. Rev.* **124** 452
[45] Garcia-Sanchez F, Borys P, Vansteenkiste A, Kim J V and Stamps R L 2014 *Phys. Rev. B* **89** 224408
[46] Ravelosona D, Cebollada A, Briones F, Diaz-Paniagua C, Hidalgo M A and Batallan F 1999 *Phys. Rev. B* **59** 4322
[47] Vansteenkiste A, Leliaert J, Dvornik M, Helsen M, Garcia-Sanchez F and Waeyenberge B V 2014 *AIP Adv.* **4** 107133
[48] Venkat G, Fangohr H and Prabhakar A 2018 *J. Magn. Magn. Mater.* **450** 34
[49] He J X and Zhang S F 2008 *Phys. Rev. B* **78** 012414
[50] Dolocan V O 2012 *Appl. Phys. Lett.* **101** 072409
[51] Nakatani Y, Shibata J, Tatara G, Kohno H, Thiaville A and Miltat J 2008 *Phys. Rev. B* **77** 014439
[52] Tserkovnyak Y, Skadsem H J, Brataas A and Bauer G E W 2006 *Phys. Rev. B* **74** 144405
[53] Seo S M, Lee K J, Yang H and Ono T 2009 *Phys. Rev. Lett.* **102** 147202
[54] Kim D Y, Berrai I, Suraj T S, Roussigné Y, Yang S H, Belmeguenai M, Hu F R, Shi G Y, Tan H R, Huang J F, Soumyanarayanan A, Kim K W, Cherif S M and Yang H 2024 *Phys. Rev. Lett.* **133** 156704